Paper 5

Tectonic processes in the Jan Mayen Fracture Zone based on earthquake occurrence and bathymetry

Sørensen, M.B., Ottemöller, L., Havskov, J., Atakan, K., Hellevang, B. and Pedersen, R.B.

Tectonic processes in the Jan Mayen Fracture Zone based on earthquake occurrence and bathymetry

Mathilde Bøttger Sørensen[1], Lars Ottemöller[2], Jens Havskov[1], Kuvvet Atakan[1],

Bjarte Hellevang[1], Rolf Birger Pedersen[1]

[1]Department of Earth Science, University of Bergen, Allegt. 41, 5007 Bergen, Norway,

[2]British Geological Survey, Murchison House, West Mains Road, Edinburgh EH9 3LA,

UK.

Abstract

Jan Mayen is an active volcanic island situated along the mid-Atlantic Ridge north of

Iceland. It is closely connected with the geodynamic processes associated with the

interaction between the Jan Mayen Fracture Zone (JMFZ) and the slowly spreading

Kolbeinsey and Mohns Ridges. In spite of the significant tectonic activity expressed by

the frequent occurrence of medium to large earthquakes, detailed correlation between

individual events and the causative faults along the JMFZ has been lacking. Recently

acquired detailed bathymetric data in the vicinity of Jan Mayen has allowed us to

document such correlation for the first time. The earthquake of April 14, 2004 (M_w=6),

which occurred along the JMFZ, was studied in detail and correlated with the

bathymetry. Locations of aftershocks within the first 12 hours after the main shock

outline a 10 km long fault plane. Interactions between various fault systems are

demonstrated through locations of later aftershocks, which indicate that supposedly normal fault structures to the north of the ruptured fault, in the Jan Mayen Platform, have been reactivated. Correlation of the waveforms shows that events located on these structures are significantly different from activity at neighboring structures. Coulomb stress modeling gives an explanation to the locations of the aftershocks but cannot reveal any information about their mechanisms.

Introduction

Jan Mayen is a volcanic island located on the northern mid-Atlantic ridge between Greenland and Norway (Figure 1a), created by the Beerenberg volcano. The area is seismically active with the occurrence of both volcanic and tectonic events [*Havskov and Atakan*, 1991]. Since 1972, a three-station seismic network has been operational on the island. Digital recording started in 1982. The present network consists of three vertical short-period seismometers and an additional 3-component broadband station (JMIC, Fig. 1b), which was installed in 2003 as part of the International Monitoring System (IMS) under the Comprehensive Nuclear-Test-Ban Treaty (CTBT).

Jan Mayen is situated between the two main spreading ridges along the North Atlantic, the Kolbeinsey ridge to the south and the Mohns ridge to the north (Figure 1a). These two mid-oceanic ridges are offset laterally by the Jan Mayen Fracture Zone (JMFZ), which approximately passes through the northernmost tip of the island. Spreading along these two main ridge systems is relatively slow at a rate of 15-17 mm/year [*Kreemer et al.*,

2003; *De Mets et al.*, 1990; *De Mets et al.*, 1994]. The island can also be described as being at the northern end of the Jan Mayen ridge which has been accepted by many as a micro-continent [e.g. *Sylvester*, 1975; *Myhre et al.*, 1984; *Kodaira et al.*, 1998] and possibly is a detached relict of the Greenland continental rise [e.g. *Johnson and Heezen*, 1967; *Talwani and Eldholm*, 1977]. North of the JMFZ, a small topographic ridge parallels the fracture zone, which develops into an approximately 60 km wide bank opposite the island [*Haase et al.*, 1996]. The Jan Mayen Platform (JMP, Figure 2) was probably generated at a northward propagating spreading axis [*Haase and Devey*, 1994]. A recent study of *Svellingen* (2004) suggests that the JMP is probably anomalously thick crust with the same petrophysical properties as the Mohns ridge and differing from the Jan Mayen island in its petrophysics. The platform spreading center has a strike parallel to the Kolbeinsey ridge while the Mohns ridge north of about 71.5°N strikes in a more easterly direction [*Haase et al.*, 1996].

The seismicity rate in the region is high with the occurrence of both tectonic and volcanic events. Figure 1b shows events with M > 3 (M_w, M_L or M_C) recorded by the Norwegian National Seismic Network (NNSN) in the time period 1972-2003. The large scatter of the events is partly caused by location uncertainties, but it is clear that activity is concentrated along the spreading axes and the JMFZ, and in the JMP. There is activity to the southwest of the island as well, but this is much more scattered. Due to the location uncertainties and limited knowledge of the detailed tectonics in the region, it has up to now not been possible to associate large earthquakes to specific fault structures. Prior to 2004, the previous large earthquake to occur in the Jan Mayen region was a M_b=5.7 event

on December 13, 1988. The location of this event is shown in Figure 1b [*Havskov and Atakan*, 1991].

In addition to tectonic earthquakes, activity has been observed in connection to eruptions of the Beerenberg volcano, most recently during the eruption in January 1985. At the early stages of this eruption, a large number of low-frequency events were recorded by the local network, with waveforms significantly different from tectonic events in the region. In addition, large tectonic events were recorded during the eruption, which are described by *Havskov and Atakan* [1991] to be triggered, but not caused, by the eruption.

The bathymetry in the neighborhood of the JMFZ and especially to the north of the island was recently mapped in a detailed survey conducted by the Norwegian Petroleum Directorate (NPD) (Figure 2). *Pedersen et al.* [in prep.] have interpreted this bathymetric dataset from the structural point of view. The lateral offset of the mid-Atlantic ridge along the JMFZ is accommodated by a left-lateral linear transform fault lying in NW-SE orientation, the Koksneset fault. To the north, the JMP is characterized by a number of NE-SW oriented structures that constitute the southwestern-most part of the submerged Mohns ridge. These structures are expected to be normal faults accommodating the extension in the JMP. Similar processes are observed elsewhere [e.g. *Cochran and Martinez*, 1988; *Kusznir and Park*, 1987; *Ebinger*, 1989].

On April 14, 2004 at 23:07 UTC, a large earthquake ($M_W = 6.0$) occurred northeast of Jan Mayen. In this study, we looked at the large amount of data available from this event and

its aftershocks together with the detailed bathymetry data to improve the understanding of the tectonic processes in the area.

The 14 April, 2004 earthquake

The main shock was located using data from the stations on Jan Mayen and the HYPOCENTER location program [*Lienert and Havskov*, 1995]. The final location was obtained using P phases from the four local stations and a low-weight S phase from station JMIC. The JMIC S phase was given a 25% weight and S phases from other stations were not included since records were saturated. The location obtained is listed together with other source parameters in Table 1. The velocity model used for locating earthquakes is that of *Sørnes and Navrestad* [1975] (Table 2), which is used by the NNSN for locating events in the Jan Mayen region. This model is based on a seismic refraction survey carried out in 1973 with 25 shot points along a profile crossing the island and in near-coastal locations around the island. Recording was done at six stations distributed on the island.

Figure 2 shows the epicenter of the event plotted on the high-resolution (50m) bathymetry map [*Pedersen et al.*, in prep.]. The event is located on the eastern segment of the Koksneset fault, which is the only fault in the vicinity capable of generating such a large earthquake. Our location of the main shock (BER) falls 9 km northeast of the location given by the Preliminary Determination of Epicenters (PDE) of the U. S. Geological Survey (Figure 1b). Since the stations are quite close to the epicenter (nearest

station at 30 km), our phase picks are sufficiently precise to give a reliable epicenter estimate. The depth of the event is not well constrained by the data, but both NNSN and PDE locations indicate a depth of 10-15 km. Theoretical arrival times based on the BER and PDE locations, using the local velocity model, show a much better fit to the data for the BER location.

The fault plane solution, as given in the Harvard CMT catalogue, is almost pure strike-slip as shown in Figure 2. This mechanism fits well with the first motion polarities recorded by the NNSN. The NW-SE striking nodal plane is in good agreement with the orientation of the Koksneset fault.

Aftershocks

The local network on Jan Mayen recorded several hundred aftershocks. We describe analysis of aftershocks that occurred during the first two months after the main shock. Within this time, a total of 110 events with local magnitude (M_L) larger than 2.7 were recorded. In Figure 3a it is seen that the daily number of events decays exponentially as predicted by Omori's law [*Utsu*, 1961] during the first 3 weeks. However, aftershock activity continues clustered in time during the following weeks. Figure 3b shows the magnitude distribution of the aftershocks located on the ruptured fault segment (see below). The cumulative magnitude frequency distribution of aftershocks, including only events located on the ruptured fault segment, gives a b-value of 1.3, which is as expected

for an aftershock sequence within the uncertainties of the magnitude determination (see e.g. *Stein and Wysession* [2003]).

The largest aftershock was recorded on April 15 at 1:11 (UTC) with a magnitude of M_w=4.0. According to Båth's law, the largest event of an aftershock sequence statistically is 1.2 magnitude units smaller than the main shock for continental events [*Felzer et al.*, 2002; *Helmstetter and Sornette*, 2003]. This predicts an aftershock, which is significantly larger than what is observed for the April 14, 2004 event. However, *Boettcher and Jordan* [2004] suggest that oceanic transform faults have strongly deficient aftershock sequences with the largest aftershocks being 2.2 magnitude units smaller than the main shock on average. Our observations are in good agreement with this suggestion.

The aftershocks were located using two different approaches for comparison. First, we located the events individually based on manually picked phase arrivals using HYPOCENTER. Second, we determined phase arrivals through cross-correaltion and located using joint hypocenter determination. Cross-correlation was also used to indentify groups of similar events.

The location of events with manually picked phases was done for earthquakes with $M_L \geq$ 2.7. The P onsets are very clear and can be read reliably with 10 ms accuracy, whereas the S-phases are more difficult to read and have an uncertainty of 10-60 ms. The same technique as used for locating the main shock was applied to the aftershocks. This means that P picks from the four local stations and a low-weight (25%) S pick from JMIC were

used. Due to the unfavorable station configuration, with event locations offshore whereas stations are on land, there is practically no depth control. Therefore the depth was fixed at 15 km, which is near the assumed thickness of the crust in the Jan Mayen region [*Sørnes and Navrestad*, 1975]. Locations were spread over a 40 km long area. Systematic station residuals were observed, which indicates lateral heterogeneities in the local velocity structure beneath Jan Mayen. Applying average corrections for station residuals, the aftershocks were concentrated in a much smaller area, about 10 km long.

It was observed that locations of aftershocks within 12 hours (early aftershocks) of the main shock are located on the mainshock rupture (Figure 2 and 4a) while later aftershocks locations are also found to the north. The early aftershocks are aligned in the WNW-ESE direction, indicating the extent of the active fault plane (box in Figure 2). This has a lateral extent of about 10 km which fits well with the expected length of the fault plane for a M = 6 strike-slip interplate event [*Wells and Coppersmith*, 1994].

First motion polarities of the aftershocks are in agreement with the main shock fault plane solution. The locations of these events also fit very well with the outline of the eastern segment of the Koksneset fault, based on the detailed bathymetry. This correlation infers that the rupture occurred along the eastern segment of the Koksneset fault. The location of the main shock falls at the northwestern end of the segment as defined by the aftershock distribution.

The later aftershocks still show significant activity on the main fault. In addition, two event clusters are seen in the JMP to the north of the mainshock.

To quantify the uncertainties associated with manual phase picking, one event was relocated using 10 sets of manual phase readings. The locations obtained varied within 2 km, which can therefore be taken to be a minimum location uncertainty. Another estimate of the location uncertainty comes from considering the spread of the aftershocks perpendicular to the strike of the ruptured fault plane. Considering both fault plane solution and bathymetry data, the dip of the fault is steep (80-90º), and we therefore expect little spread of the aftershocks perpendicular to the fault. In Figures 2 and 4 it is seen that the early aftershocks are distributed over a ca 5 km wide zone, and this may be a reasonable estimate of the actual location uncertainty.

As second approach, we determined phase arrivals by applying a waveform cross-correlation technique [*Schaff and Richards*, 2004]. We determined absolute arrival times through correlation with selected master events as described by *Ottemöller* [2005]. The phase arrival is given by the maximum amplitude in the correlation function and absolute arrival time is obtained in relation to the manual phase reading on the master signal. A time window of 1.5 sec around the phase arrival was used and the waveform data were filtered in the frequency band 3-6 Hz. We determined P arrivals for all stations on Jan Mayen and S arrivals from the broadband data only. We also used cross-correlation as a measure to identify groups of similar events.

The phase arrivals determined through cross-correlation were used to locate the events by joint hypocenter determination (JHD). The VELEST program [*Kissling et al.*, 1994] was used for the JHD, inverting for event locations simultaneously while keeping the velocity model fixed. In total, 162 aftershocks were studied with the correlation technique including events with $M_L \geq 2.2$ for the early aftershocks and events with $M_L \geq 2.7$ for the later aftershocks.

The cross-correlation technique revealed five groups of events with similar waveforms and a remaining number of uncorrelated events. The resulting locations for the individual groups are shown in Figure 4b. Three groups (groups 1-3) are clearly associated with the eastern segment of the Koksneset fault. The remaining two groups (groups 4-5) are located on the assumed normal faults to the north within the JMP. There is no clear temporal grouping of these events, except that groups 2 and 3 occur mainly within 24 hours after the main shock. The events of groups 4 and 5 within the JMP belong to different sources, as indicated by different P-wave polarities as well as their location.

The locations obtained from the two techniques are similar (Figure 4). The spread in location of groups 1, 3, 4 and 5 based on cross-correlation data appears to be similar or slightly smaller than for locations based on manual picks. Some of the events in group 2 are off the mainshock rupture, possibly due to poor readings based on the cross-correlation. The two clusters north of the mainshock rupture from cross-correlation and JHD are shifted several kilometers towards the northeast compared to the manual locations. We consider the manual locations more reliable with respect to the absolute

location of the events. Using different velocity model/station corrections in the two techniques may explain the mismatch in the locations. Manual inspection has shown that the manual phase readings are more precise regarding the absolute arrival times.

Tectonic interpretation

Most earthquakes along the JMFZ have strike-slip mechanisms with one of the nodal planes parallel to the fracture zone [*Havskov and Atakan*, 1991]. The earthquake of April 14, 2004 is the most recent example of this trend. Both the Harvard and the USGS moment tensor solutions indicate an almost pure strike-slip mechanism with one of the nodal planes aligned along the orientation of the JMFZ. Moreover, the location of the event coincides well with the Koksneset fault (Figure 2), providing the first observation of direct association between an earthquake epicenter and a fault in the area. The alignment of the aftershocks along the same trend delineates the extent of the actual fault segment that ruptured during the April 14 event, which has a length of approximately 10 km.

The majority of the later aftershocks occurred on assumed normal faults within the JMP. The activation seems to be associated with two distinct clusters which correlate well with transfer zones oblique to the general NE-SW trending lineaments of the JMP. These are expected zones of weakness, and are probably activated as oblique normal faults with a right-lateral strike-slip component.

In order to test this hypothesis, the coulomb stress change caused by the main shock was calculated using the Coulomb software [*Toda et al.*, 1998]. A horizontal slip of 0.3 m along a fault with 10 x 10 km dimensions and strike and dip from the fault plane solution was assumed. In addition, the regional stress orientation was assumed to be $\sigma_1=0°$ (vertical), $\sigma_2=21°$ and $\sigma_3=111°$ based on the orientation of the Koksneset fault. The coulomb stress change was calculated both for optimally oriented normal faults and for optimally oriented strike-slip faults as shown in Figure 5. In addition to the coulomb stress change, locations of aftershocks within two months after the main shock are shown. The two clusters of events in the JMP are located in a region where the coulomb stress has increased for both normal and strike-slip faults. In this regard, the modeling does not help us in resolving the most probable mechanism for the events, but it provides important information about why the reactivation occurs in that particular region. Another interesting feature observed in Figure 5 is that all aftershocks near the western end of the ruptured fault plane occur in a region with increased coulomb stress for optimally oriented strike-slip faults and reduced coulomb stress for optimally oriented normal faults, supporting that these events must have strike-slip mechanisms as indicated by the tectonics.

The observed polarities of the events in the JMP support the hypothesis that the mechanisms of these events are normal or oblique. For the clusters of events located on the faults within the JMP, all waveforms have positive P-wave polarity. This is as one would expect for a normal fault dipping eastwards in the given geometry because all

stations are located on the foot-wall side of the fault. The aftershocks on the Koksneset fault, on the other hand, have negative P-wave polarities, as does the main shock.

The previous large earthquake to occur in the Jan Mayen area (December 13, 1988, M_b = 5.7) was located in the same region as the present event and had a similar fault plane solution [*Havskov and Atakan*, 1991]. The first 10 aftershocks of the 1988 and 2004 events were relocated using the same stations and phases for all events. Both sets of aftershocks occupied the same area within a couple of kilometers and the relative arrival times of P phases from the recent event and the 1988 event on the Jan Mayen stations were identical within 0.01 s, which indicates that both events have ruptured the same segment of the Koksneset fault. Both these earthquakes, with similar magnitudes, have occurred along the same segment of the Koksneset fault, only 16 years apart. This raises the question of whether such events occur regularly, and if so, what the recurrence interval is. Looking at the seismicity in the region during the last century indicates recurrence times of 10-20 years for events of $M \geq 6$ in the region. The accumulated strain along the entire JMFZ, based on the spreading rate of 15-17 mm/year, is sufficient to generate earthquakes of this size with a recurrence interval of 7-9 years assuming slip values based on *Wells and Coppersmith* [1994], but it is difficult to establish a precise recurrence interval, which also depends on the degree of coupling on the fault. Assuming full coupling, the expected recurrence interval for events of M=6 along a 10x10 km fault patch for a range of stress drops was calculated, assuming a spreading rate of 16 mm/yr and that slip scales as the square root of the rupture area (*Margaret Boettcher*, personal communication, 2006). The results indicate that a recurrence interval of 10-15 years

would give full seismic coupling on a fault patch for earthquakes with stress drops of 0.5-1 MPa, which is in the range of stress drops found on ridge transform faults (*Margaret Boettcher*, personal communication, 2006; *Boettcher and Jordan*, 2004; *Boettcher*, 2005). This is an interesting result because it implies that a particular fault patch is fully coupled, while the surrounding fault area is probably slipping predominantly aseismically. The largest instrumentally recorded earthquake in the region was a M_s=6.5 event in 1923, however, considering the length of the Koksneset fault, larger events up to M = 7.5 may be possible.

A comparable deformation to that of the Jan Mayen Fracture Zone is found along the South Iceland Seismic Zone, where the offset of the Reykjanes ridge occurs on land through a series of en-echelon fault segments oriented in the north-south direction. In this area, several clusters of earthquakes have occurred along these NS oriented faults during 282 years giving rise to the estimated average seismic moment release of 2.3×10^7 Nm/year [*Hackman et al.*, 1990]. This rate, however, is 1.4 times larger than the expected average rate (approximately 1.65×10^7 Nm/year) based on the case where all the deformation occurs along a straight transform fault [*MacDonald et al.*, 1986]. The JMFZ is analogous to the latter case where deformation is accommodated by a straight transform fault, similar to fast-spreading ridges. The total seismic moment rate along the JMFZ, therefore, indicates similar values and is found to be compatible with the estimated strain rate based on the GPS data [*Kreemer et al.*, 2003; *De Mets et al.*, 1990; *De Mets et al.*, 1994].

Conclusions

In this study we have addressed the geodynamic processes occurring along the plate margin in the North Atlantic through the study of a recent significant earthquake and its aftershocks. Although the April 14, 2004 Jan Mayen earthquake is a single event in the entire ongoing deformational processes, it provides important clues about the details of earthquake processes on ridge transform faults. Detailed investigations on the tectonic style of the area [*Pedersen et al.*, in prep.] have delineated individual structures capable of generating large earthquakes. Previous observations based on seismological data only were not sufficient to associate individual earthquakes in the region with specific fault structures. In this study we have presented for the first time evidence for such a correlation.

The largest fault in the area is the Koksneset fault, which strikes NW-SE along the eastern part of the JMFZ. This fault is shown to be the origin of the 14 April 2004 and 13 December 1988 earthquakes, and probably also of earlier large events. The aftershocks of the 14 April, 2004 event confirmed a rupture length of about 10 km. Two additional clusters with different source mechanisms from the main shock were triggered further north, indicating readjustments of the neighboring structures.

This earthquake provided the most recent evidence of the ongoing activity along the Jan Mayen Fracture Zone and helps us to understand better the deformational processes along this plate boundary in the North Atlantic.

Acknowledgements

References

Boettcher, M.S. and Jordan, T.H. (2004), Earthquake scaling relations for mid-ocean ridge transform faults, *J. Geophys. Res.*, *109*, B12302, doi:10.1029/2004JB003110.

Boettcher, M.S. (2005), Slip on Ridge Transform Faults: Insights from Earthquakes and Laboratory Experiments, Ph.D. thesis, Massachusetts Institute of Technology and Woods Hole Oceanographic Institution.

Cochran, J.R. and Martinez, F. (1988), Structure and tectonics of the northern Red Sea: catching a continental margin between rifting and drifting, *Tectonophysics*, *150*, 1-32.

DeMets, C., Gordon, R.G., Argus, D.F. and Stein, S. (1990), Current plate motions, *Geophys. J. Int.*, *101*, 425-478.

DeMets, C., Gordon, R.G., Argus, D.F. and Stein, S. (1994), Effect of recent revisions to the geomagnetic reversal time scale on estimates of current plate motions, *Geophys. Res. Lett.*, *21*, 2191-2194.

Ebinger, C.J. (1989), Tectonic Development of the Western Branch of The East African Rift System, *Geological Society of America Bulletin*, *101*, 885-903.

Felzer, K.R., Becker, T.W., Abercrombie, R.E., Ekström, G. and Rice, J.R. (2002), Triggering of the 1999 M_w 7.1 Hector Mine earthquake by aftershocks of the 1992 M_w 7.3 Landers earthquake, *J. Geophys. Res., 107*(B9), 2190, doi:10.1029/2001JB000911.

Haase, K.M. and Devey, C.W. (1994), The petrology and geochemistry of Vesteris Seamount, Greenland Basin – an intraplate alkaline volcano of non-plume origin, *J. Petrol.*, *35*, 295-328.

Haase, K.M., Devey, C.W., Mertz, D.F., Stoffers, P. and Garbe-Schönberg, D. (1996), Geochemistry of lavas from Mohns Ridge, Norwegian-Greenland Sea: implications for melting conditions and magma sources near Jan Mayen, *Contrib. Mineral Petrol.*, *123*, 223-237.

Hackman, M.C., King, G.C.P., and Bilham, R. (1990), The mechanics of South Iceland Seismic Zone, *J. geophys. Res.*, *95*, 17339-17351.

Havskov, J. and Atakan, K. (1991), Seismicity and volcanism of Jan Mayen Island, *Terra Nova*, *3*, 517-526.

Helmstetter, A. and Sornette, D. (2003), Båth's law derived from the Gutenberg-Richter law and from aftershock properties, *Geophys. Res. Lett.*, *30*(20), 2069, doi:10.1029/2003GL018186.

Johnson, G.J. and Heezen, B.C. (1967), Morphology and evolution of the Norwegian Greenland Sea, *Deep-Sea Res.*, *14*, 755-771.

Kissling, E., Ellsworth, W.L., Eberhart-Phillips, D. and Kradolfer, U. (1994), Initial reference model in local earthquake tomography, *J. Geophys. Res*., *99*, 19635-19646.

Kodaira, S., Mjelde, R., Gunnarsson, K., Shiobara, H. and Shimamura, H. (1998), Structure of the Jan Mayen microcontinent and implications for its evolution, *Geophys. J. Int.*, *132*, 383-400.

Kreemer, C., Holt, W.E., and Haines, A.J. (2003), An integrated global model of present-day plate motions and plate boundary deformation, *Geophys. J. Int.*, *154*, 8-34.

Kusznir, N.J. and Park, R.G. (1987), The extensional strength of the continental lithosphere: its dependence on continental gradient, and crustal composition and thickness, in *Continental Extension Tectonics,* 28**,** edited by Coward, M.P., Dewey, J.F. and Hancock, P.L., pp. 35–52, Geol. Soc. Lond., London.

Lienert, B.R.E. and Havskov, J. (1995), A computer program for locating earthquakes both locally and globally, *Seism. Res. Lett., 66*, 26-36.

MacDonald, K.C., Castillo, D.A., Miller, S.P., Fox, P.J., Kastens, K.A. and Bonatti, E. (1986), Deep tow studies of the Vema Fracture Zone 1: Tectonics of a major slow

slipping transform fault and its intersection with the Mid-Atlantic Ridge, *J. Geophys. Res.*, *91*, 3334-3354.

Myhre, A., Eldholm, O. and Sundvor, E. (1984), The Jan Mayen Ridge: Present Status, *Norsk Polar Inst. Skr.*, *2*, 47-59.

Ottemöller, L. (2005), Improvement of earthquake location in the UK using correlation techniques, IASPEI General Assembly, Santiago, Chile.

Pedersen R.B. Svellingen, W. and Hellevang, B. (in prep), The submarine geology of the Jan Mayen region: A unique example of ridge-transform-micro continent interaction. (manuscript in prep.).

Schaff, D. P., and P. G. Richards (2004), Repeating seismic events in China, Science, 1178, 303:1176-1178.

Stein, S. and Wysession, M. (2003), *An introduction to seismology, earthquakes, and earth structure*, pp. 277, Blackwell Publishing, Oxford.

Svellingen, W. (2004), Submarin vulkanisme i Jan Mayen området, M.Sc. thesis, Department of Earth Science, University of Bergen.

Sylvester, A.G. (1975), History and surveillance of volcanic activity on Jan Mayen island, *Bull. Volcanol.*, *39*, 1-23.

Sørnes, A. and Navrestad, T. (1975), Seismic survey of Jan Mayen, *Norsk Polar Inst. Årbok*, 37-52.

Talwani, M. and Eldholm, O. (1977), Evolution of the Norwegian-Greenland Sea, *Bull. Geol. Soc. Am.*, *88*, 969-999.

S. Toda, R. S. Stein, P. A. Reasenberg and J. H. Dieterich (1998), Stress transferred by the Mw=6.9 Kobe, Japan, shock: Effect on aftershocks and future earthquake probabilities, *J. Geophys. Res., 103*, 24,543-24,565.

Utsu, T. (1961), A statistical study on the occurrence of aftershocks, *Geophys. Mag., 30*, 521-605.

Wells, D.L. and Coppersmith, K.J. (1994), New empirical relationships among magnitude, rupture length, rupture area and surface displacement, *Bull. Seism. Soc. Am. 84*, 974-1002.

Tables

Table 1: Source parameters of the April 14, 2004 Jan Mayen earthquake. Location is obtained by this study, M_0: Seismic moment (PDE), M_w: Moment magnitude (PDE), M_s: Surface wave magnitude (PDE), Fault plane solution is from the Harvard CMT database and I_{max}: Maximum intensity (Reported to UiB).

Date	14/4 2004
Time (UTC)	23:07:39.2
Latitude	71.093°N
Longitude	-7.472°E
Depth	10.5 km
M_0	10^{18} Nm
M_w	6.0
M_s	5.6
1st nodal plane:	
Strike	111°
Dip	87°
Rake	2°
2nd nodal plane:	
Strike	21°
Dip	88°
Rake	177°
I_{max}	V

Table 2: Velocity model used by NNSN for locating earthquakes in the Jan Mayen area. $V_p/V_s = 1.73$ in the model. From *Sørnes and Navrestad* [1975].

Depth (km)	V_p (km/s)
0-18	6.33
18-50	7.90
50-80	8.25
80-	8.50

Figure captions

Figure 1.

a) Location of Jan Mayen in the North Atlantic. The dots are earthquakes with magnitude 4 or larger recorded by ISC in the time period 1990-1999. The black box outlines the area in Figure 1b. It is seen that the seismicity clearly outlines the mid-Atlantic ridge. b) Earthquakes in the Jan Mayen region in the time 1972-2003. The seismic stations on Jan Mayen are shown as triangles together with the April 14, 2004 event located as determined in this study (BER, star) and by USGS (PDE, circle) and the December 1988 event (diamond).

Figure 2.

Earthquake locations plotted on the bathymetry. The locations of the Koksneset fault and the spreading axis (as located by *Pedersen et al.* [in prep.]) are indicated on the map. Contour lines are altitudes (in m) on Jan Mayen. The Jan Mayen Platform is located north of the Koksneset fault. The 14 April, 2004 main shock is shown with the fault plane solution from the Harvard CMT catalogue. The blue dots are aftershocks occurring within 12 hours after the main shock; the red dots are later aftershocks occurring within 2 months after the main shock. The box outlines the extent of the ruptured fault plane from the aftershock distribution. A and B mark the two clusters of events within the JMP, which are expected to occur on normal faults.

Figure 3.

Aftershock statistics for the April 14, 2004 Jan Mayen earthquake. a) Daily distribution of aftershocks with $M_L \geq 2.7$ for the first two months after the main shock. b) Magnitude distribution of aftershocks on the ruptured fault segment with $M_L \geq 2.7$. The bars show the number of aftershocks of a given magnitude (M_w); the line shows the cumulative number of aftershocks above a given magnitude.

Figure 4.

Comparison of aftershock locations using the two techniques. a) Aftershock locations obtained with manual phase picks as in Figure 2. The blue dots are events within 12 hours after the main shock, the red dots are later events occurring within two months after the main shock. b) Aftershock locations obtained using the correlation technique. Different colors represent groups of events with correlated waveforms. The main shock is shown with fault plane solution from the Harvard CMT catalogue.

Figure 5.

Coulomb stress change caused by the April 14, 2004 Jan Mayen earthquake for a) optimally oriented normal faults and b) optimally oriented strike-slip faults. The white line indicates the location of the fault plane in the model, and black circles are aftershocks within the first 2 months after the main shock, located manually.
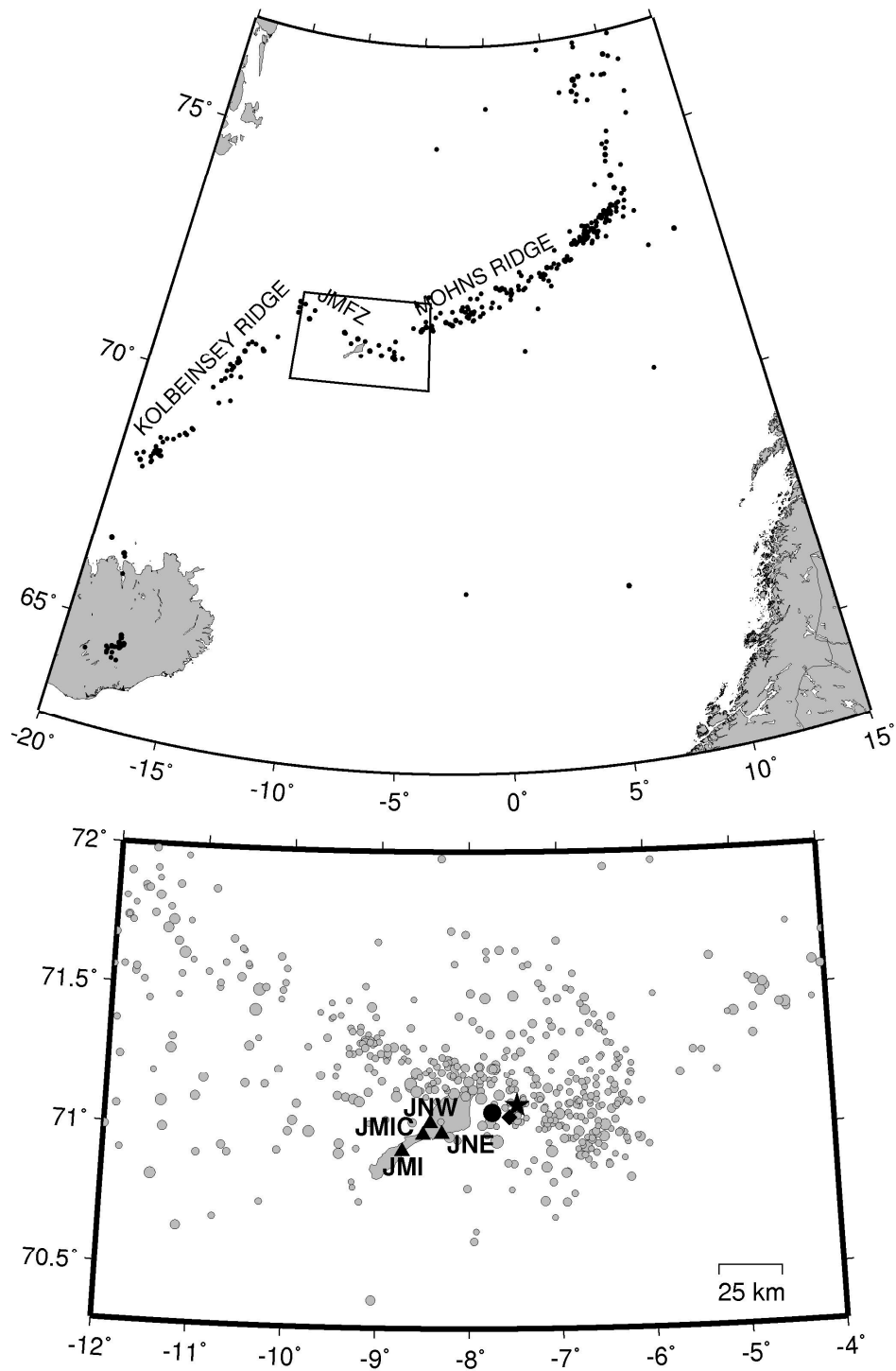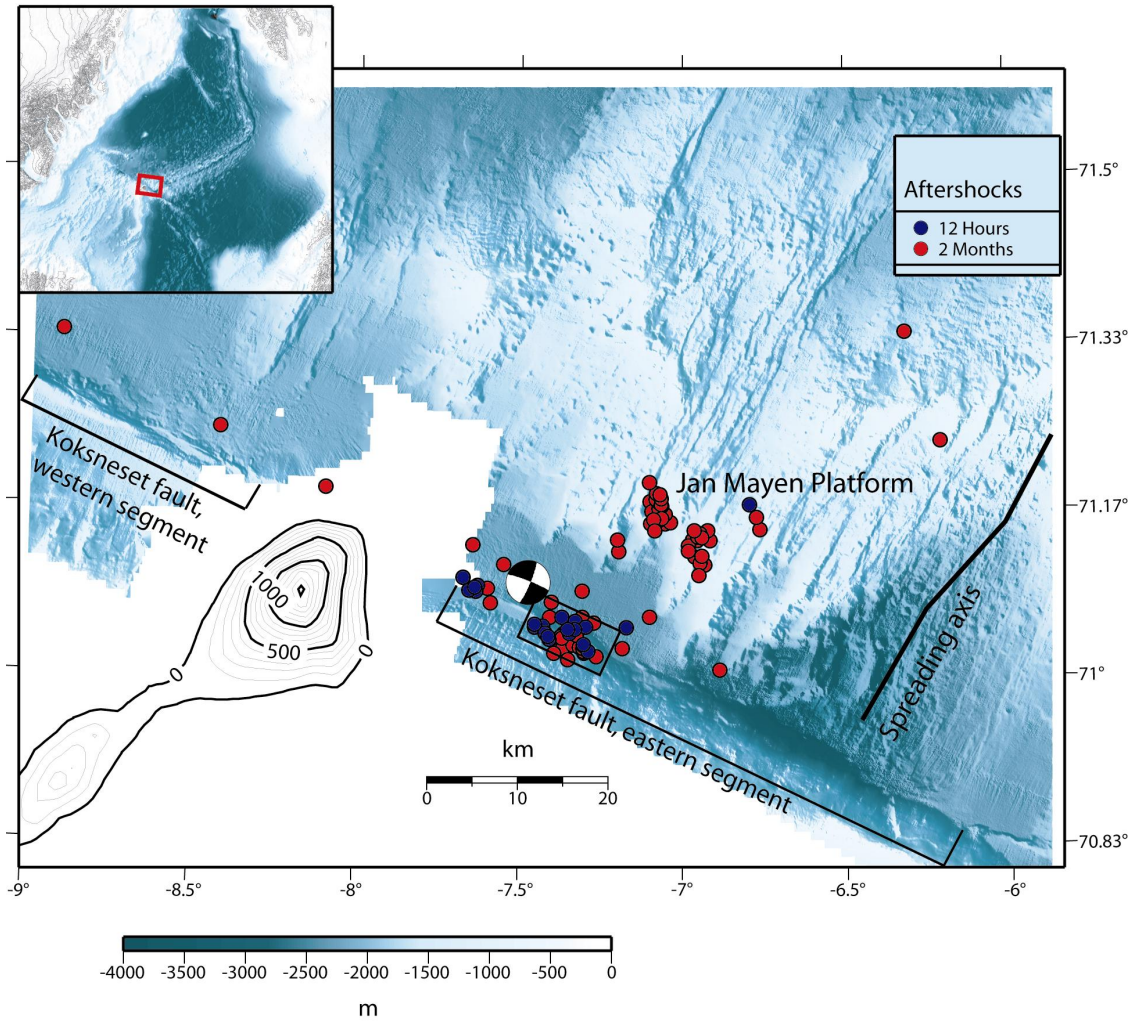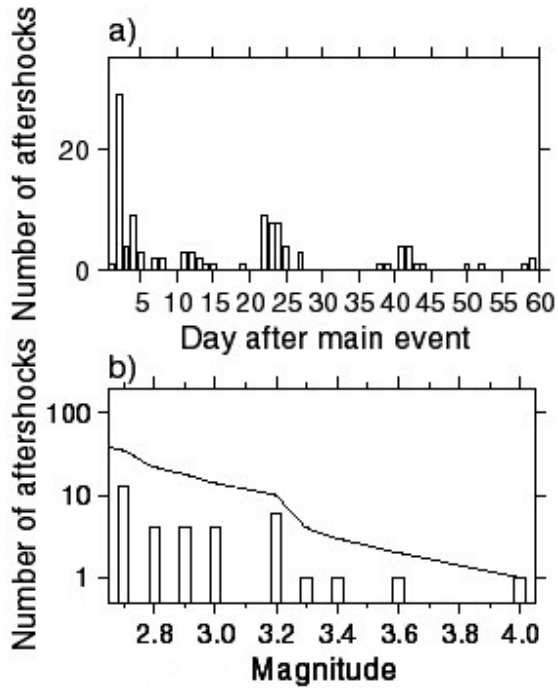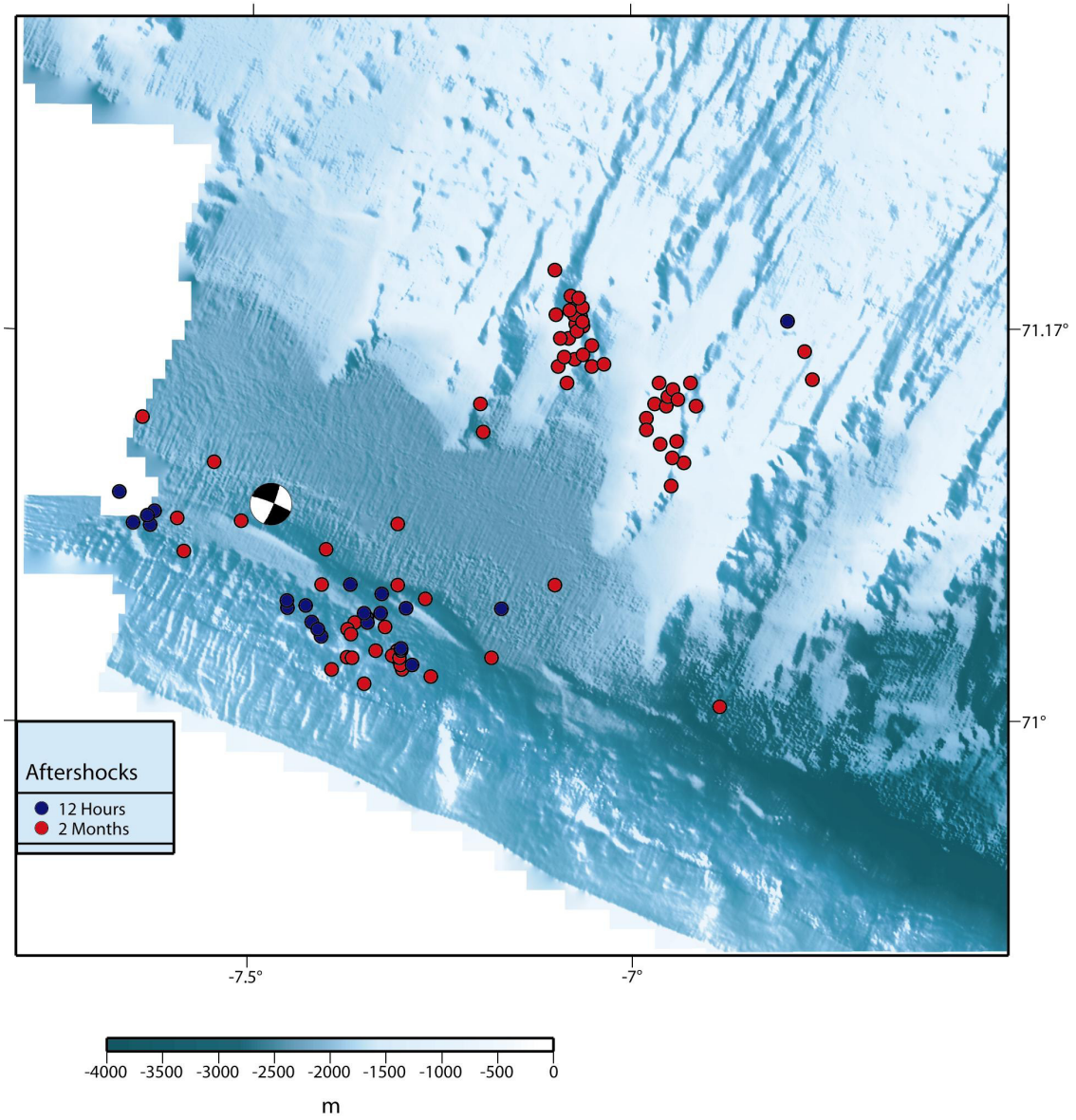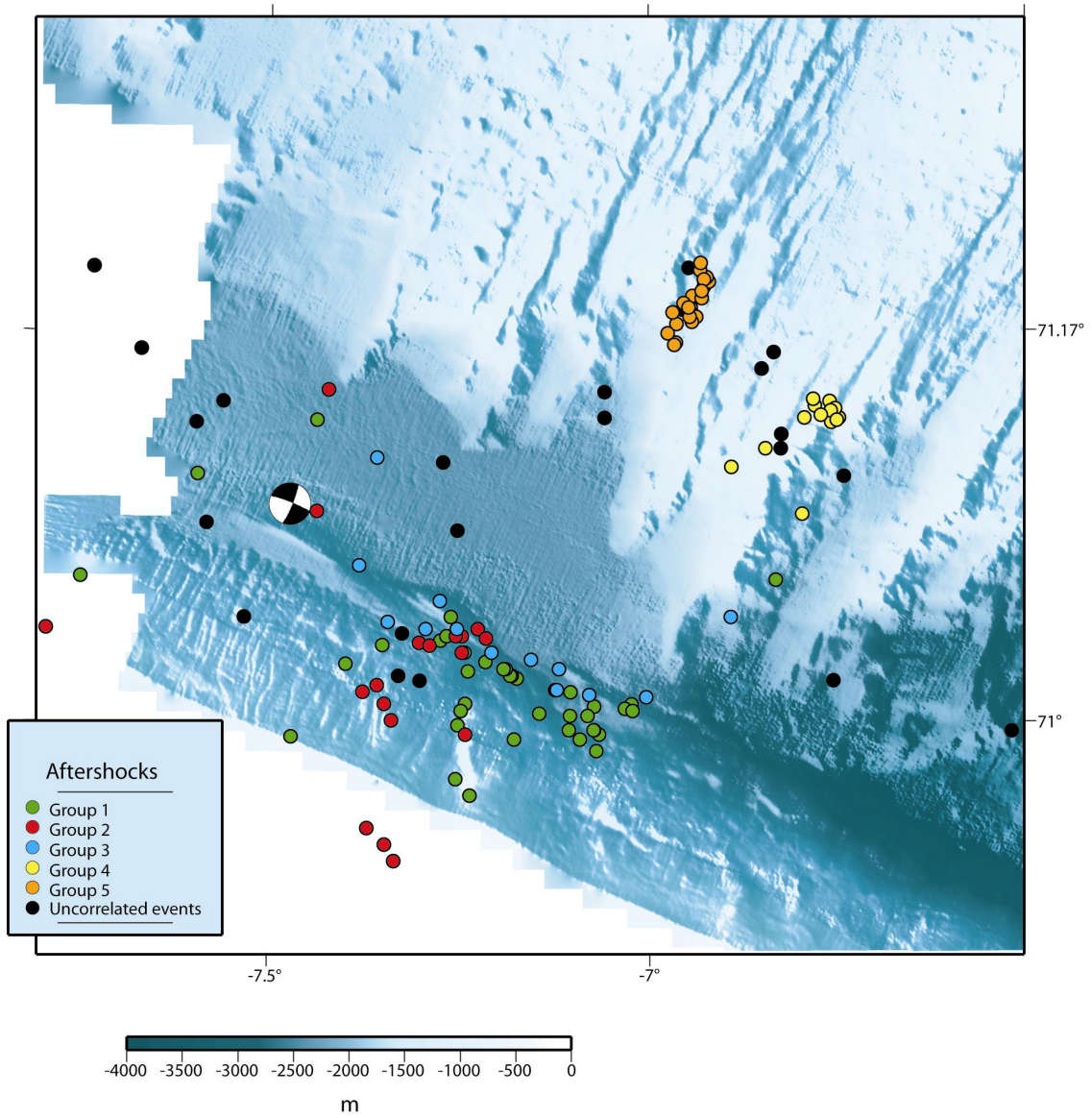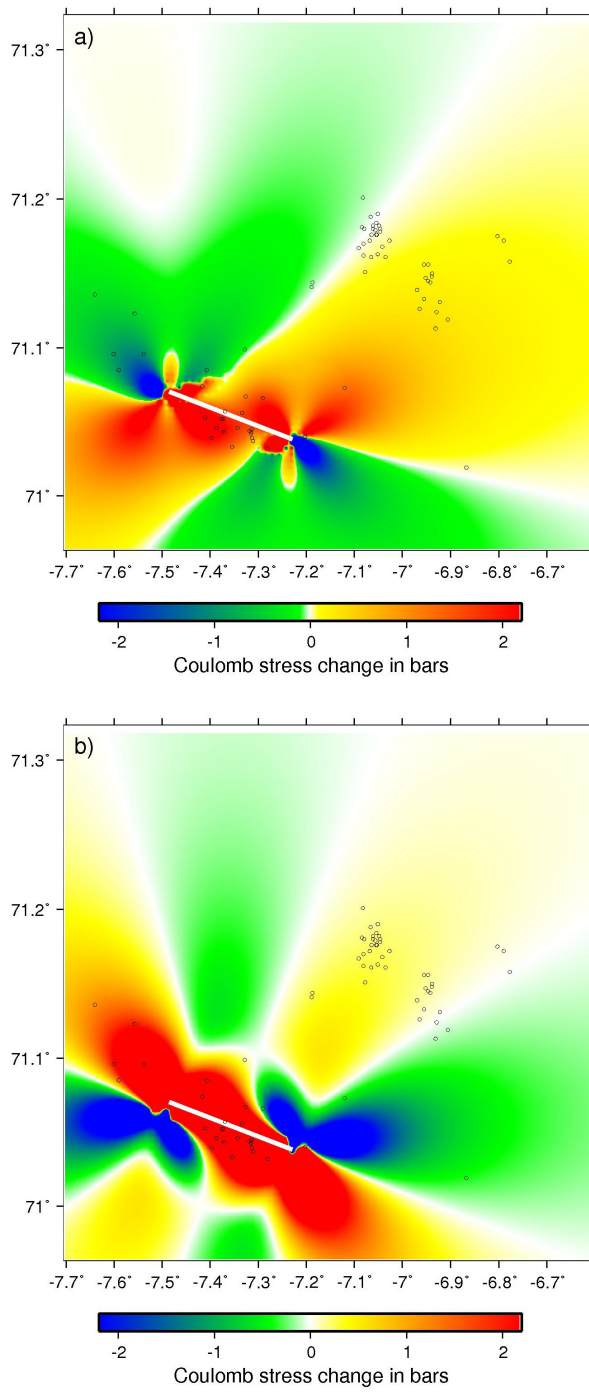
Figure 1

Figure 2.

Figure 3.

Figure 4a

Figure 4b.

Figure 5.